Heliyon 10 (2024) e27224

Contents lists available at ScienceDirect

Heliyon

journal homepage: www.cell.com/heliyon

Research article

High-intensity pulsed-light cultivation of unicellular algae: Photosynthesis continues in the dark

Yair Zarmi

Jacob Blaustein Institutes for Desert Research, Ben-Gurion University of the Negev, Midreshet Ben-Gurion, 8499000, Israel

ARTICLE INFO

Keywords:
Unicellular algae
High photon-flux
Pulsed-light regime
PS II photosynthetic efficiency

ABSTRACT

Experiments have shown that photon exploitation efficiency in unicellular algal biomass production under a pulsed-light regime with a high-photon flux is higher than the efficiency under continuous illumination with the same flux. This observation has been explained theoretically to be a consequence of the improved efficiency of exploitation of photons by Photosystem II (PS II) thanks to the combined effect of photon-absorption statistics, a rate-limiting time scale and the size of the PQ pool.

Exploiting the same ideas, it is shown in this paper that, under a pulsed-light regime, there is a pulse-time length, for which the average exploitation efficiency of PS II absorbed photons is maximal. Under ideal conditions, this maximum is close to 100%. The optimal pulse-time length is roughly proportional to the size of the PQ pool, N_{PQ}. This is clearly seen for τ (the average time gap between consecutive photons absorbed by the PS II-Chlorophyll antenna) of the order of 1 ms or less (corresponding to a high photon flux and/or a large photon absorption cross-section area of the antenna) and for small N_{PQ}. The width of the plot of efficiency vs. pulse length around the optimum is then small and the optimal pulse length is well defined. As τ is increased beyond 1 or N_{PQ} becomes large, the width grows, allowing for a broad choice of pulse lengths, for which efficiency is very close to the maximum.

These observations open the door to future designs of highly productive bioreactors.

1. Introduction

Unicellular algae offer an important biomass source for humanity. Being the simplest plants, many researchers have focused for decades, and still do, on the study of the characteristics of the algal photosynthesis. The photosystem functions through a large number of chemical reactions and diffusion processes, involving a large number of biomolecules. Despite the complexity, the overall functional performance of the photosystem can be described by a "block diagram" [see, e.g., [1–10]]: The first stage (Photosystem II, or PS II) absorbs photons. The energy of these photons is exploited to energize electrons, which are delivered to the next stage (Photosystem I, or PS I), where additional photons are absorbed. The energy of the absorbed photons serves as the driving force for the generation of biomolecules of importance for the organism.

The focus of this paper is algal biomass production under pulsed-light regime at high photon fluxes. An increase in photosynthetic efficiency under a pulsed-light regime at high photon fluxes relative to the efficiency under continuous illumination at the *same* high photon flux was first observed in strongly mixed, high-density cultures [11–13]. Owing to the random motion of cells between the illuminated and the dark layers, cells were, effectively, exposed to short light pulses (of the order of 0.1–1 ms). Later on, an increase in

E-mail address: zarmi@bgu.ac.il.

https://doi.org/10.1016/j.heliyon.2024.e27224
Received 14 August 2023; Received in revised form 15 December 2023; Accepted 26 February 2024
Available online 7 March 2024

biomass productivity under pulsed-light regimes was observed in pulsed light experiments on unicellular algae [14–21] and on macro-algae [22].

The observations of Refs. [15,18and21] were explained theoretically to be a consequence of the improved efficiency of exploitation of photons by PS II thanks to the combined effect of photon-absorption statistics, a rate-limiting time scale and the size of the PQ pool [21]. However, these experiments did not perform detailed scanning of the light-pulse length, Hence, they could not find whether an optimal pulse time existed, for which efficiency is maximal. In this paper it is shown that, for given biological parameters, under ideal conditions, there is a pulse-time length, for which PS II photosynthetic efficiency under pulsed-light regimes can be close to 100% for any high photon flux. It will be also found that the optimal light-pulse duration is close to being proportional to the size of the PQ pool of PS II. This may play a significant role in the future design of high-productivity bioreactors.

The basic tenet is that, under a high-flux pulsed-light regime, photosynthesis can continue for a while during the dark time that follows a pulse. This leads to a PS II photosynthetic efficiency that is higher then the efficiency under continuous illumination at the *same* high flux. The energy of some of photons absorbed by the Chlorophyll antenna of PS II can be delivered directly to PS I through an electron transfer process during the pulse time. The energy of additional absorbed photons is stored in the PQ pool, and delivered to PS I during the dark time that follows a pulse, leading to the increase in the photosynthetic efficiency.

For clarity, the ideas first presented in Ref. [21] are reviewed here in detail.

2. Continuous illumination

2.1. Rate-limiting time scale of 10 ms

Under continuous irradiation of algal cultures, it is customary to plot three plots, in each case a quantity is plotted vs. photon flux. These are: Oxygen rate (oxygen P–I curve), biomass-production rate (biomass P–I curves) (see, e.g., Refs. [23,24]) and PS II to PS I transfer rate of energized electrons (ETR curves [5,25–31]). All three curves flatten off at about the same photon fluxes (above 150–300 μmol/m^2/s). Over the saturation branch of P–I curves, photon exploitation efficiency goes down in inverse proportion to the applied flux. For example, at a flux of 1000 μmol/m^2/s (about half a full sun), the energy of only 10–20% of photons in the photosynthetically active range (the photon wavelength range exploited by the photosystem) is exploited. Consequently, under full sunlight, the energy of just a few percent of impinging photons is exploited.

The observation that all three curves (P–I curves of O_2 and biomass production and ETR curves) turn over to saturation at about the same photon fluxes imply.

1) All three processes are affected by one and the same rate-limiting time scale, which has been estimated to be of the order of 10 ms [21]. As the statistical distribution of this time scale is not known, the estimated 10 ms will be used. Saturation implies that the photosystem can process the energy of at most one photon every 10 ms. The obvious question is what the origin of this rate-limiting time scale is.
2) All three curves are proportional to one another (at least approximately). Of significance for the purpose of this paper is the proportionality between biomass P–I curves and ETR curves:

$$P_{biomass} = K\ ETR. \tag{1}$$

The constant K may depend on growth conditions.

ETR is the average PS II → PS I delivery rate of energized electrons. As such, it is just $r^{PS\ II}_{exp\ loited}$, the average rate, at which PS II-absorbed photons are exploited. Hence, Eq. (1) can be also written as:

$$P_{biomass} = K\ r^{PS\ II}_{exploited}. \tag{2}$$

On top of the technical proportionality, Eq. (2) conveys a message of deeper significance: **The average biomass production rate is proportional to the average rate of exploitation of PS II-absorbed photons.**

This interpretation means that all one has to do is count photons that are exploited by PS II. It is the fundamental starting point to the discussion of pulsed-light regimes in the following.

2.2. Another 10 ms rate-limiting time scale

Absorption of two photons by PS II leads to the splitting of a water molecule and the release of an Oxygen atom. Four photons are, therefore, required for generating one O_2 molecule. The energy of a photon is exploited in a sequence of rapid excitation processes that end up with the storage of energized electrons in (each by the energy of a single photon) pairs by the reduction of a Plastoquinone molecule (PQ), the reduced state denoted by PQ^{-2}. Energized electrons are then delivered one-by-one from PS II to PS I. The process starts with the "release" of an energized electron through a rapid multi-step process, summarized by

$$PQ^{-2} \rightarrow PQ^{-1} + e. \tag{3}$$

This is followed by a much slower diffusion process through cell membranes.

τ_{del}, the delivery time of an energized electron from PS II to PS I, has been estimated to be of the order of 10 ms [31–35]. This estimate is corroborated by the analysis of ETR data (see, e.g., Refs. [5,23–28]). The statistical distribution of τ_{del} is not known. In the

lack of better knowledge, the estimate of 10 ms is adopted.

2.3. Two rate-limiting time scales are one and the same?

The preceding discussion, in particular, Eq. (2), leads to the suggestion that the rate-limiting time scales estimated from the dependence on photon flux of P–I curves (Section 2.1) and the that of PS II → PS I energized electron transfer (Section 2.2) are one and the same.

This is puzzling, and still not understood, regarding, at least, two aspects. First, the rate-limiting time scale of O_2 generation is also 10 ms despite the fact that this process occurs *prior* to energized-electron transfer to PS I. This requires that a (feedback?) mechanism exists, which limits O_2 generation when photons are absorbed by the Chlorophyll antenna of PS II at a rate that exceeds one photon every 10 ms.

No less puzzling is the fact that biomass generation occurs far later on in the production line through the collective effect of many photons and much longer rate-limiting time scales, of the order of hundreds of ms and more. Already in PS I, the exploitation of the energy of absorbed photons involves longer rate-limiting time scales (e.g., the Calvin cycle – 300 ms). None of these long time scales seem to affect the photon flux dependence of biomass generation (P–I curve) or the electron transfer rate (ETR curve). The only rate-limiting time scale is 10 ms. Based on theses observations, it is suggested that saturation is a result of the fact that the delivery of electrons, each energized through the absorption of a single photon, from PS II, to PS I, occurs successively, at most, one electron every 10 ms.

While confirmation and understanding of these ideas are still missing, their adoption implies that the biomass generation rate is determined primarily by the average exploitation rate of photons absorbed by PS II (see Eq. (2)). Hence, the rest of this paper focuses on this exploitation rate.

2.4. Biomass production rate and 10 ms rate-limiting time scale

Given that energized electrons can be delivered only in 10 ms steps, when the photon flux is high so that the PS II-photon absorption rate exceeds one photon every 10 ms, the energy of excess photons cannot be delivered directly to PS I. The energy of some photons can be stored in the energy storage component of PS II by twice reducing each PQ molecule ($PQ \rightarrow PQ^{-2}$) in the PQ pool. Denoting the number of PQ molecules in the PQ pool by N_{PQ}, up to ($2\ N_{PQ}$) energized electrons can be stored. The energy of excess photons is lost. N_{PQ} may have a statistical distribution [31–34,36]. Its magnitude has been estimated to be about of 5–12 with an average of about 7.

Under high continuous photon fluxes, which lie in the saturation branch of a P–I curve, the PQ pool plays no role in determining photosynthetic efficiency because all PQ molecules in the energy storage are doubly reduced all the time. Consequently, as observed experimentally, the photosynthetic efficiency falls off in inverse proportion to the photon flux absorbed by the Chlorophyll antenna of PSII because the exploitation rate is constant: one photon every 10. With $r^{PS\ II}_{exploited}$ denoting the exploitation rate of PS II absorbed photons one obtains an estimate of the efficiency under continuous illumination, $\eta_{PS\ II}$, continuous:

$$\begin{aligned} r^{PS\ II}_{exploited,Continuous} &= 0.1\ photons \Big/ ms \Rightarrow \\ \eta_{PS\ \ II,Continuous} &= (0.1\ photons/ms) \Big/ (n_0\ photons/ms) \end{aligned} . \tag{4}$$

n_0 is the average rate of photon absorption per ms by the chlorophyll antenna of PS II. The conventional units for the photon flux, I_0, are μmol/m^2/s. Conversion into the desired units of photons/ms is given by

$$n_0 = C\ I_0\ A \quad (C = 0.000602215). \tag{5}$$

A, the photon-absorption cross-section area of the antenna in nm^2 is of the order of 1 nm^2 [37–48]. Thus, the efficiency goes down like $1/(I_0)$.

3. High PS II efficiency under pulsed light

It has been observed that, under high photon fluxes (on the saturation branch of the biomass P–I curve), photon-exploitation efficiency in biomass production under exposure to judiciously chosen light-pulse regimes is 3–10 times higher than under continuous illumination using the *same* high fluxes in three types of experiments.

1) High-density cultures exposed to continuous illumination. Light penetrates only through a very thin layer of the culture. Turbulence induced in the fluid forces cells to undergo a random walk, leading to effective exposure to light-dark cycles [11–13].
2) Low-density cultures (to a good approximation, all cells subjected to same photon flux) exposed to artificially generated light-dark cycles [14–21];
3) Exposure of Macro-Algae to light pulses [22].

In the framework proposed here, these observations imply that (see Eq. (2)), out of the total number of photons absorbed by the Chlorophyll antenna of PS II during a light pulse, the average fraction of photons, the energy of which is exploited, is higher than the fraction exploited under continuous illumination; photosynthesis continues during the dark time following the pulse.

Based on the ideas reviewed above, the results of measurements on low-density cultures [15,19and21] as well as the construction of a P–I curve for continuous illumination data were given a simple quantitative explanation using a numerical simulation program [21]. It was suggested that the PQ pool in PS II comes into play. Some electrons, each energized by the absorption of one photon, may be delivered to PS I directly during the pulse (one electron every 10 ms). Additional electrons, also energized during the pulse, can be stored in pairs in the PQ pool, two in twice-reduced Plastoquinone molecules (PQ^{-2}). Energized electrons stored in the PQ pool can then be delivered to PS I also during the dark time.

Photon energy is wasted when n_{abs}, the number of photons absorbed by the Chlorophyll antenna of PS II during a pulse, is so large that

$$n_{abs} \geq N_{10} + (2N_{PQ}). \tag{6}$$

N_{10} is the number of energized electrons delivered during the pulse in 10 ms steps:

$$N_{10} = \left[T_p \,/\, 10\right] + \theta\left(T_p \;-\; 10\,\left[T_p \,/\, 10\right]\right) \quad \left(\theta(x) = \begin{cases} 1, x > 0 \\ 0, x < 0 \end{cases}\right). \tag{7}$$

The square brackets represent the integer part of (T_p/10). The first term is the number of 10 ms steps, each corresponding to the delivery of one electron. As T_p is usually not an integer product of 10 ms, the second term accounts for the delivery of one more electron in the "tail" beyond a full set of 10 ms steps.

n_{abs} may obey Eq. (6) under any combination of three factors: a high photon flux, long pulse duration and a large photon absorption cross-section area of the Chlorophyll antenna of PS II. When Eq. (6) is obeyed, (2 N_{PQ}) energized electrons are stored in the PQ pool. All PQ's in the pool are doubly reduced. There is no room for additional energized electrons. The energy of the excess photons is wasted.

4. Optimal pulse duration

In the following it is shown that, under a pulsed-light regime, given the photon absorption cross-section area of the Chlorophyll antenna of PS II (of the order of 1 nm^2), the size of the PQ pool and the number of energized electrons stored in the PQ pool at the beginning of a pulse, under the best scenario, there is an optimal pulse duration, for which PS II photosynthetic efficiency is close to 100% for any high photon flux.

The unknowns are many. Of particular importance is the number of energized electrons stored in the PQ pool at the beginning of a light pulse. This number depends on the length of the dark time preceding the beginning of the next pulse – whether it has been sufficiently long for delivering as many energized electrons stored in the PQ pool in the previous light-dark cycle as possible. It may also depend on the lifetime for the loss of energized electrons by the decay of PQ^{-2} and/or PQ^{-1} molecules in the PQ pool and, perhaps, other unknown factors. Hence, this note studies several simple scenarios. Examination of the results presented in the following requires the performance of light-pulse experiments with low-density cultures, so that, within a good approximation, all cells are exposed to the same light intensity.

5. Photon statistics

Light pulses are generated nowadays by lasers or LED's. n_{abs}, the number of photons absorbed during one pulse of length, T_p, varies randomly. The probability for the absorption n_{abs} photons during a pulse follows a Poisson distribution [49,50], given by:

$$P\left(n_{abs}, T_p, \tau\right) = \frac{\left(T_p/\tau\right)^{n_{abs}}}{n_{abs}!}\, e^{-\left(T_p/\tau\right)}. \tag{8}$$

τ, the average time gap between two consecutive photons, is given in ms by

$$\tau = \frac{1}{n_0} = (1 \,/\, (C\, I_0\, A)), \tag{9}$$

where n_0 is defined in Eq. (5). Note that what counts is the average time gap between consecutive photons: A given value of τ may correspond to different photon fluxes, I_0, and A, the photon absorption cross-section areas by the PS II antenna.

Under the probability distribution, Eq. (8), the average number of photons absorbed during a single pulse and the standard deviation are:

$$\langle n_{abs}\rangle = \left(T_p \,/\, \tau\right), \sigma = \sqrt{\langle \eta_{ph}{}^2\rangle \;-\; \langle \eta_{ph}\rangle^2} = \sqrt{\left(T_p/\tau\right)}. \tag{10}$$

Photon statistics plays a crucial role in analyzing measured data: As light pulses of relevance are of the order of a few ms, $<n_{abs}>$ is small, just a few photons. For example, for a photon flux of 1000 μmol/m^2/s and a photon absorption cross-section area of 1 nm^2, Eq. (9) yields τ = 1.66 ms. Hence, by Eq. (10), the average number of photons absorbed during a 10 ms pulse is 6 and the standard deviation is 2.45.

Eq. (10) yields statistically significant information regarding the spread of the results around the average only when $<n_{abs}> \gg 1$, for which the law of large numbers applies and the probability function of Eq. (8) approaches a Gaussian. When $<n_{abs}>$ is small (O(1) or less), the value of the standard deviation in Eq. (10) does not represent the correct spread. It only yields an idea about the order of

magnitude of the spread.

6. Rate-limiting time scale of 0.2 ms

A rate-limiting time scale, estimated to be about 0.2 ms, affects the generation process of a PQ^{-2} molecule in PS II [5,48]. If the time gap between the two consequent photons required for the excitation of two electrons is too short, then the second photon is wasted, and the system has to wait for the next photon. In the simplified calculations presented in the following, events, in which the number of photons absorbed during a pulse is so large that the average time gap between consecutive photons is 0.2 ms or less will not be included in the statistical evaluation. These are events for which

$$n_{abs} \geq N_{0.2} = \left[T_p \,/\, 0.2\right] + 1, \tag{11}$$

The square brackets represent the integer part of (T_p/0.2).

7. Energy delivery from PS II to PS I

At this stage, the computation focuses on what happens during a single pulse. N_{10} energized electrons (see Eq. (7)) are delivered from PS II to PS I during the pulse, one every 10 ms. Energized electrons stored in the PQ pool are delivered during the following dark time. Denoting the number of energized electrons stored in the PQ pool during a pulse by n_{stored}, in the most desired scenario, all but one are delivered to PS I during the dark period following the light pulse. The last electron remains in the pool in a PQ^{-1} (a consequence of Eq. (3)). Hence, in the best scenario, the number of photons, the energy of which is delivered during one light-dark cycle is

$$n_{delivered} = N_{10} + n_{stored} \quad - \quad 1. \tag{12}$$

Eq. (12) implies that the largest number of photons, the energy of which can be delivered to PS I during one light-dark cycle, is,

$$n_{stored} = 2\, N_{PQ} \Rightarrow \max n_{delivered} = N_{10} + 2\, N_{PQ} \quad - \quad 1. \tag{13}$$

If n_{abs}, the number of photons absorbed by PS II during a pulse, exceeds the maximum given in Eq. (13), then the number of energized electrons delivered to PS I remains as in Eq. (13). The energy of excess photons is wasted.

In Section 8, photon exploitation is calculated for a given value of n_{abs}, the number of photons absorbed by the Chlorophyll antenna of PS II during one pulse. The computation of the number of exploited photons, averaged over many light-dark cycles, is accounted for in Section 9, exploiting the probability of Eq. (8).

8. Photon-energy exploitation

8.1. Most desired scenario

In the most desired scenario discussed above, one energized electron, left from the previous light-dark cycle, is stored in the PQ pool at the beginning of the next light pulse. As long as n_{abs} obeys (see eq. (11))

$$n_{abs} \leq N_{10} + (2N_{PQ}) \quad - \quad 1 \tag{14}$$

and provided that the dark time following the light pulse is long enough, n_{exp}, the number of exploited photons (the number of energized electrons (each energized by a single photon) delivered to PS I) is:

$$n_{exp} = n_{abs}. \tag{15}$$

Once the bound of Eq. (14) is exceeded, the number of delivered energized electrons remains at Eq. (14). (The energy of excess photons is lost.) Hence one then has:

$$n_{exp} = N_{10} + 2\, N_{PQ} \quad - \quad 1, \tag{16}$$

n_{exp} grows linearly with n_{abs} for low values of n_{abs}, and goes into saturation when

$$n_{abs} > N_{10} + (2N_{PQ}) \quad - \quad 1 \tag{17}$$

8.2. Other scenarios

Worse scenarios emerge if, following a complete light-dark cycle, n_{left}, the number of energized electrons left in the PQ pool at the beginning of a new pulse is not 1.

8.2.1. Most desired scenario with loss of energy of last electron – $n_{left} = 0$

Consider the possibility that, in case of the most desired scenario, discussed in Section 8.1, the energy of the single energized electron left in the PQ pool in a PQ^{-1}, is lost owing to the decay of the PQ^{-1} into PQ + *e*., so that $n_{left} = 0$. The next light pulse then begins with no energized electrons left in the PQ pool. As long as n_{abs} obeys

$$n_{abs} \leq N_{tot} = N_{10} + (2N_{PQ}), \tag{18}$$

the energy of all energized electrons, but one, is delivered to PS I. Hence, Eq. (15) for exploited the number of PS II-absorbed photons is modified into

$$n_{exp} = n_{abs} - 1. \tag{19}$$

Again, it grows linearly with n_{abs}. Once n_{abs} equals or exceeds the maximum value allowed by Eq. (18), $n_{\exp}$ reaches saturation.

8.2.2. $N_{left} > 1$ scenario

$n_{left} > 1$ may emerge if the dark time is too short (preventing the delivery of all stored energized electrons but one to PS I before the beginning of the next light pulse). It may depend on the lifetime for the loss of energized electrons by PQ^{-1} and PQ^{-2} molecules left in the PQ pool at the end of one cycle and other, still unknown, causes. This slightly modifies the calculation of the dependence of $n_{\exp}$, the number of exploited PS-II absorbed photons on n_{abs}. However, the qualitative picture is the same as in the two scenarios of $n_{left} = 0$ and 1. The reason is that $n_{left} > 1$, effectively, corresponds to reduction of the size of the PQ pool. Fig. 1 shows the dependence of $n_{\exp}$ on n_{abs} for scenarios with $n_{left} = 1$, 0 and 5, $T_p = 20$ ms and $N_{PQ} = 7$. One sees that $n_{left} > 1$ is tantamount to reducing the storage capacity of the PQ pool.

9. Efficiency averaged over many light-dark cycles

Averaging over all values of n_{abs}, using the probability function of Eq. (8), the number of exploited photons as a function of n_{abs} (Eqs. (15) and (16), or Eqs. (19) and (16), or appropriately modified expressions for $n_{left} > 1$) yields $< n_{\exp} >$, the number of exploited photons during one pulse, T_p, averaged over many light-dark cycles, each with a different value of n_{abs}, the number of absorbed photos:

$$\langle n_{exp} \rangle = \sum_{n_{abs}=2}^{N_{low}} P(n_{abs}, T_p, \tau) \cdot n_{exp,low} + \theta(N_{0.2} - N_{high}) \sum_{n_{abs}=N_{high}}^{N_{0.2}} P(n_{abs}, T_p, \tau) \cdot n_{exp,high}. \tag{20}$$

In Eq. (20), $n_{\exp,low}$ is number of absorbed photons (depending on the scenario, Eqs. (15) or (19)), which is sufficiently low, so that all are exploited. $n_{\exp,\ high}$ denotes the number of exploited photons for a high number of absorbed photons. These two entities as well as N_{low} and N_{high} will be defined for each scenario. Averaging is performed over events with different values of n_{abs}, the number of photons absorbed by PS II during a pulse.

9.1. Most desired scenario ($n_{left} = 1$)

The most desired scenario, $n_{left} = 1$, corresponds to a situation, in which the energy of all energized electrons stored in the PQ pool, except for one, remaining in a single PQ^{-1}, has been either delivered to PS I, or has been wasted. In this case,

$$\begin{array}{c} n_{exp,low} = n_{abs}, n_{exp,high} = N_{tot} - 1 \\ N_{low} = \min(N_{tot} - 1, N_{0.2} - 1), N_{high} = N_{tot} - 1 \end{array}. \tag{21}$$

N_{tot} is defined in Eq. (18).

9.2. $n_{left} \neq 1$ scenarios

The case $n_{left} = 0$ occurs when the energy of the single energized electron left in the PQ pool is lost owing to the decay of the

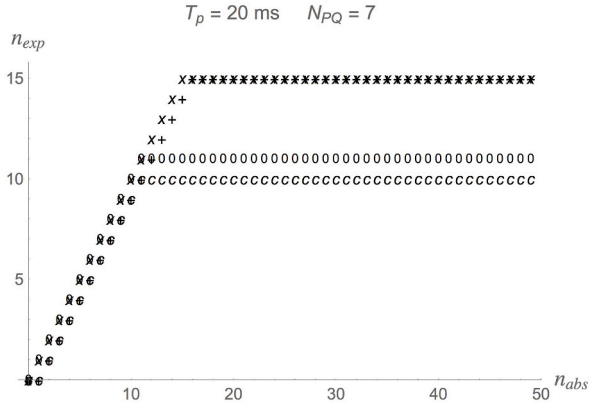

Fig. 1. Number of exploited photons vs. number of photons absorbed during a pulse. $T_p = 20$ ms, $N_{PQ} = 7$, for different scenarios. x: $n_{left} = 1$; +: $n_{left} = 0$; 0: $n_{left} = 5$, all absorbed photons exploited; c: $n_{left} = 5$, all absorbed photons but one exploited.

remaining PQ^{-1}. One then has:

$$\begin{aligned} n_{exp,low} &= n_{abs} - 1, n_{exp,high} = N_{tot} - 1 \\ N_{low} &= \min(N_{tot}, N_{0.2}), N_{high} = N_{tot} \end{aligned} \tag{22}$$

When $n_{left} > 1$, one subtracts n_{left} from N_{tot}, defined in Eq. (18).

Fig. 2 shows the average number of exploited photons, $<n_{\exp}>$, vs. the pulse length, T_p, for $N_{PQ} = 5$, $\tau = 1$ ms and $n_{left} = 1$, where Eq. (21) has been used. The dashed straight line is $<n_{abs}>$. The purpose of this Figure is to demonstrate that there is a range of values of T_p, over which the average number of exploited photons is very close to the average number of absorbed photons (Namely, the PS II photosynthetic efficiency is close to 100%. The case of $n_{left} > 1$ (Eq. (22)) is not discussed any further, because, as stated in Section 8.2.2, $n_{left} > 1$ is tantamount to reducing the storage capacity of the PQ pool.

Figs. 3–6, show plots of the average PS II photosynthetic efficiency, $\eta PULSE$ vs. T_p, for different values of N_{PQ} and, τ. $\eta PULSE$ is given by:

$$\eta PULSE = \sum_{n_{abs}=2}^{N_{low}} P(n_{abs}, T_p, \tau) \cdot \frac{n_{exp,low}}{n_{abs}} + \theta(N_{0.2} - N_{high}) \sum_{n_{abs}=N_{high}}^{N_{0.2}} P(n_{abs}, T_p, \tau) \cdot \frac{n_{exp,high}}{n_{abs}}. \tag{23}$$

Eq. (23) requires some explanation. It is the average of efficiencies, each corresponding to one event, in which n_{abs} photons were absorbed in a pulse. In each of the two sums, the efficiency of photon exploitation in an event is the fraction of exploited photons over the total number of absorbed photons.

The small spikes in the plots are artifacts of the use of a constant value of τ_{del}, the delivery time of energized electrons from PS II to PSI. They represent the jump in efficiency when the pulse duration, T_p, is increased by another step of $\tau_{del} = 10$ ms. Had the statistical distribution of τ_{del} been known, accounting for it in a more sophisticated calculational procedure would have smoothed out these spikes..

10. Optimal pulse time

Figs. 3–6 show that, given a value of τ (the average time interval between two contiguous photons, see Eq. (9)), there is an optimal pulse time. Intuitively, one might expect that $T_{p,\ optimal}$ should be proportional to ($2\ N_{PQ}$), the maximal electron- (hence, photon-energy) storage capacity of the PQ pool. However, the effect of the probability distribution of absorbed photons (Eq. (8)) leads to $T_{p,\ optimal}$ that is about 50% of the intuitive expectation.

The computed results for the optimal pulse time are shown in Fig. 7 vs. N_{PQ} (the PQ pool size), for $\tau = 1$ ms. While a rigorous mathematical derivation has not been found, the numerical results indicate that

$$T_{p,optimal} \approx N_{PQ}\ \tau. \tag{24}$$

This may serve as a good starting point for the experimental search for $T_{p,\ optimal}$.

The empirical observation of Eq. (24) requires some explanation. N_{PQ} is the number of PQ molecules in the PQ pool, and each can store two energized electrons (namely, the energy of two absorbed photons). Hence, naively, one would expect $T_{p,\ optimal}$ to be twice the result of Eq. (24):

$$T_{p,optimal} \approx 2\ N_{PQ}\ \tau. \tag{25}$$

However, owing to the effect of the probability distribution, Eq. (8), which falls off drastically at large numbers of absorbed photons,

$$n_{abs} \gg (T_p / \tau), \tag{26}$$

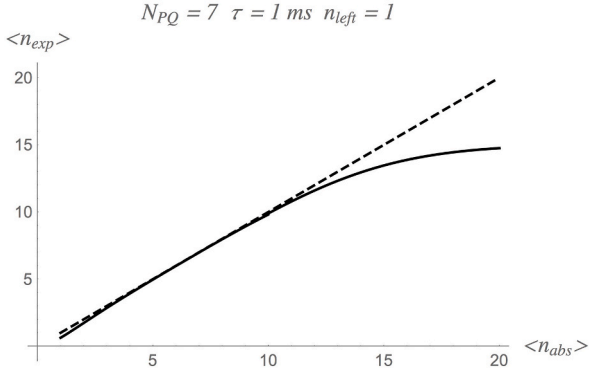

Fig. 2. $<n_{\exp}>$, average number of exploited photons under pulse-light regime vs. $<n_{abs}>$, average number of PS II- absorbed photons under pulse-light regime (Eq. (20)), $N_{PQ} = 5$, $n_{left} = 1$. Dashed line: $<nabs>$.

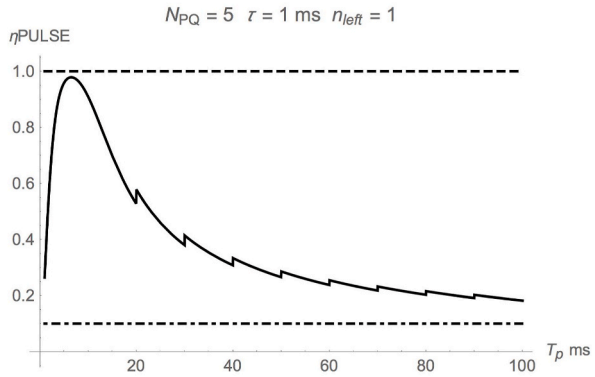

Fig. 3. *ηPULSE*, average PS II photosynthetic efficiency (Eq. (23)) under pulse-light regime: $N_{PQ} = 5$, $\tau = 1$ ms and $n_{left} = 1$.

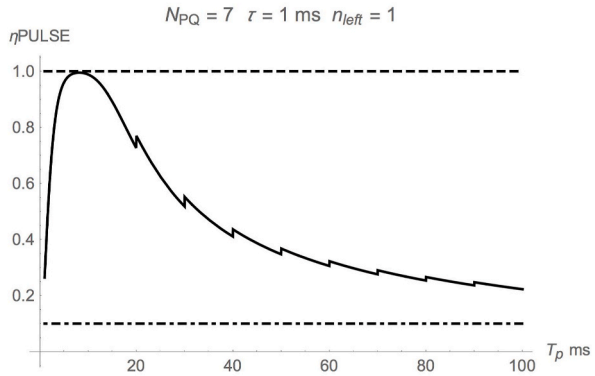

Fig. 4. *ηPULSE*, average PS II photosynthetic efficiency (Eq. (23)) under pulse-light regime: $N_{PQ} = 7$, $\tau = 1$ ms and $n_{left} = 1$.

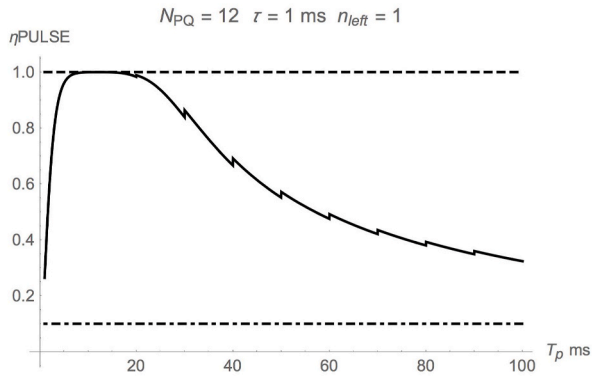

Fig. 5. *ηPULSE*, average PS II photosynthetic efficiency (Eq. (23)) under pulse-light regime: $N_{PQ} = 12$, $\tau = 1$ ms and $n_{left} = 1$.

the contribution of large values of n_{abs} is reduced leading to the smaller result of Eq. (24).

Figs. 3–5, for which τ is equal to 1 ms, demonstrate the effect of N_{PQ}, the size of the PQ pool. For small values to moderate values of N_{PQ}, the curves are narrow and the optimum is rather well defined; the resulting optimal pulse time clearly follows Eq. (24), as shown in Fig. 7. For large values of N_{PQ}, the optimum is broad and allows for a wide range of values of the pulse length, T_p, over which the efficiency is very close to optimal. Fig. 6 shows that the same effect emerges as τ is increased (plotted for $\tau = 3$ ms). The latter can be induced by reducing I_0, the photon flux, or A, the photon absorption cross-section area of the PS II Chlorophyll antenna (see Eq. (9)).

11. Efficient bioreactors

The important message of Figs. 2–6 is that, for any value of τ, (a combination of light intensity and PS II Chlorophyll antenna cross-

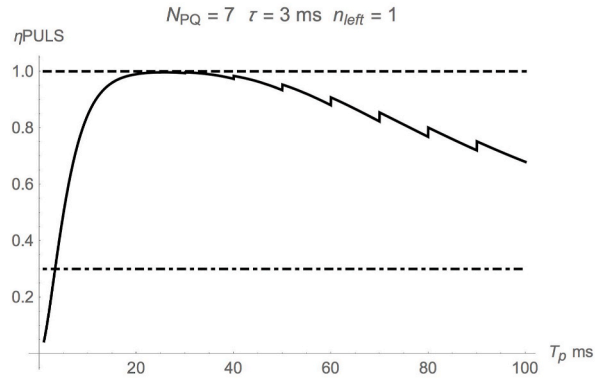

Fig. 6. *ηPULSE*, average PS II photosynthetic efficiency (Eq. (23)) under pulse-light regime: $N_{PQ} = 7$, $\tau = 3$ ms and $n_{left} = 1$.

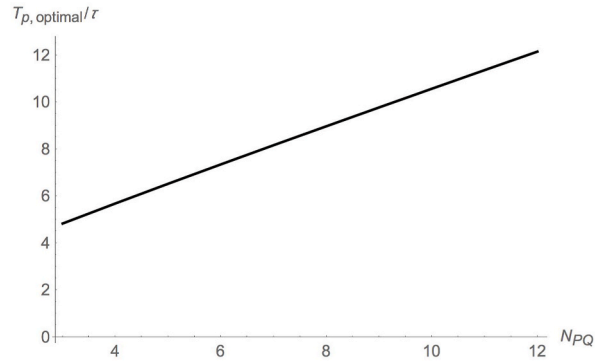

Fig. 7. ($T_{pulse,\ optimal}/\tau$) vs. size of PQ pool.

section area) there is an optimal pulse length and a range around that optimal value, for which the average PS II photosynthetic efficiency is close to 100%. This means that it is possible to design highly productive bioreactors.

Even if the actual numbers are not as high as the model presented here predicts, owing to either simplifications assumed in the model or to non-ideal conditions, the conclusion is that, for a judicious choice of the pulsed light regime, biomass production can be extremely efficient in terms of PS II photon-energy exploitation.

To be conservative, rather than discussing the optimistic results generated by the model, consider the result of Ref. [19], where it was found that for a photon flux, $I_0 = 1200$ μmol/m^2/s, the biomass production rate under a pulse regime of $T_p = 10$ ms and a dark time of 90 ms, was almost equal to the rate under continuous illumination with the *same* flux. Namely, photon exploitation efficiency was 10 times higher under the pulsed-light regime. Thus, if one divides the bioreactor surface area into 10 sectors and illuminates them sequentially by 10 ms pulses at the *same* high photon flux, one would get a total biomass production that is 10 times higher than the production under continuous illumination of the whole bioreactor by the *same* total photon energy input.

12. Optimal dark time

In low-culture density experiments, for the specific alga studied and the light pulse durations used (5, 10 and 15 ms), it has been found that there is an optimal dark time of about 200–300 ms, for which the photosynthetic efficiency under pulsed light is maximal [21]. This has also been the order of magnitude of the average dark time in the best case in the random motion of cells in the high-density experiments of [11–13]. A similar optimal dark time is obtained in a multi-parameter fit to data [51]. At present, there are no other experiments that have addressed this question. Furthermore, biological understanding for the need for an optimal dark time and what factors affect it does not exist yet.

13. Deviations from results under ideal conditions?

It is definitely conceivable that the predictions for photon exploitation efficiency may be less optimistic than the ones presented in previous Sections, where ideal conditions were assumed. However, at present, research at the most fundamental level does not provide us with the required knowledge regarding factors that may affect the actual highest possible average PS II-photosynthetic efficiency.

An example of factors, which may affect the prediction and lower PS II-photosynthetic efficiency below the optimistic (close to)

100%, is a combination of the time required to deliver to PS I an energized electron, stored in a PQ^{-2} that resides in the PQ pool, and the lifetime of PQ^{-2} (the average time it takes PQ^{-2} to lose an electron).

The time for direct delivery of an energized electron from PS II to PS I, used in previous sections, has been estimated to be of the order of 10 ms. Is the time for the delivery of an energized electron from the PQ pool to PS I similar? Are the delivery times of energized electrons from different PQ^{-2}'s that reside in the PQ pool all the same? Denote the average time it takes a PQ^{-2} to lose an electron by τ_{PQ} and the average time-gap between the delivery of an energized electron from a PQ^{-2} stored in the PQ to PS I and the delivery of the next electron by t_w. The size of the PQ^{-2} population averaged over many PQ pools, and many light-dark cycles is reduced by the typical factor of Quantum-Mechanical decay of an excited system for each "waiting time":

$$PQ^{-2}\text{population reduction} = e^{-\left(t_w/\tau_{PQ}\right)}. \tag{27}$$

For an optimal dark time of about 300 ms [19], yielding 10 ms $< t_w <$ 50 ms. The decay process is slow [1–10], hence, $500 \leq \tau_{PQ} \leq$ 3000 ms was assumed. A reduction of the high PS II photosynthetic efficiency from about 100% down to 60–90% is found from Eq. (27). If τ_{PQ} is larger, the reduction in efficiency is smaller. If τ_{PQ} is smaller, the reduction may be more significant. Still, the results are independent of the high photon flux used, hence, correspond to efficiencies that are much higher than under continuous illumination.

14. Concluding comments

The simple picture depicted in this paper leads to the conclusion that, at high photon fluxes, the photosynthetic efficiency of algal biomass production under high-intensity pulsed-light regimes may be very high, significantly higher than under continuous illumination at the same high fluxes. In view of the approximations made for the purpose of simplifying the exposition, the numerical values obtained in more detailed calculations and/or measurements may be slightly but not too different.

There are quite a few unknown or yet unexplained aspects that need to be clarified. Some have been discussed in Sections 1 and 2. Of these, the main question is why all the long time scales, which characterize biomass generation, are not rate limiting in the photon flux dependence of biomass production rates (P–I curves). Another important issue is the lack of qualitative and quantitative understanding of the required dark time that follows a light pulse.

Figs. 2–6 tell us that, for any value of τ, the average time gap between two consecutive photons, or, equivalently, any value of $n_0 = 1/\tau$ (the photon absorption rate by the PS II Chlorophyll antenna) there is a range of pulse times, for which PS II photosynthetic pulsed-light efficiency is close to 100% for any high photon flux. Thus, operating under a judiciously chosen pulsed-light regime, one can exploit the energy of a sizable fraction of the impinging photons. This means that, to get a higher photon exploitation rate in biomass production it pays to increase n_0, for example, by increasing the photon flux. Under traditional reactor operation (continuous illumination), high intensity would lead to photo-damage and photoinhibition. While there is not sufficient knowledge of this issue, it seems that this does not seem to happen under pulsed light [11–21]. A possible explanation is that in all these experiments the "duty cycle" is low, in the range of 0.01–0.3. Under such a circumstance, the average (sometimes called "integrated") light intensity is so low that it lies in the range of intensities, for which photoinhibition does not emerge.

The substantially higher photosynthetic efficiency of a pulsed-light regime (compared to that achieved under continuous illumination) does not ensure that the overall productivity of a single pulsed-light algal bioreactor is higher than that of a continuously irradiated reactor, simply because quite a lot of the production time is wasted over the dark periods between pulses (the "duty cycle", the fraction of illumination time out of the total operation time is low, often, much lower than 100%). However, the higher photosynthetic efficiency under a pulsed-light regime opens the door to the design of new highly efficient bioreactors. An example was provided in Section 10.

To find whether an optimal pulse time exists and see whether the photon-exploitation efficiency is, indeed, exceptionally high, experiments of the kind performed in Refs. 14–21 will need to be repeated, this time allowing for scanning a range of pulse times.

Finally, in the analysis presented in this paper, it is assumed that all cells are exposed to the same photon flux. Practically, this means low-density cultures. Work on the extension of the ideas to high-density bioreactors is in progress and will be published in due course.

Funding

The author declares that no funds, grants, or other support were received during the preparation of this manuscript. The author has no relevant financial or non-financial interests to disclose.

Author responsibility

1) The author made all contributions to the conception or design of the work. No data acquisition was required. No new software was created;
2) The author drafted the work or revised it critically for important intellectual content;
3) The author approved the version to be published;
4) The author agrees to be accountable for all aspects of the work in ensuring that questions related to the accuracy or integrity of any part of the work are appropriately investigated and resolved.

Data availability statement

Data sharing is not applicable to this article, as no datasets were generated or analyzed during the current study. No data associated with this study have been deposited in a publicly available repository. No data were used for the research described in the article.

CRediT authorship contribution statement

Yair Zarmi: Writing – review & editing, Writing – original draft, Software, Methodology, Investigation, Formal analysis, Conceptualization.

Declaration of competing interest

The authors declare that they have no known competing financial interests or personal relationships that could have appeared to influence the work reported in this paper.

Appendix A. Supplementary data

Supplementary data to this article can be found online at https://doi.org/10.1016/j.heliyon.2024.e27224.

References

[1] A.W.D. Larkum, J. Barret, Light-harvesting processes in algae, Adv. Bot. Res. 10 (1983) 1–219, https://doi.org/10.1016/S0065-2296(08)60260-8.
[2] G. Ananyev, G.C. Dismukes, How fast can Photosystem II split water? Photosynth. Res. 84 (2005) 355–365, https://doi.org/10.1007/s11120-004-7081-1.
[3] H.L. MacIntyre, J.J. Cullen, Using Cultures to Investigate the physiological Ecology of microalgae, ch. 19, in: R.A. Andresen (Ed.), Algal Culturing Techniques, Academic Press, 2005, pp. 287–326.
[4] A. Laisk, L. Nedbal, Govindjee (Eds.), Photosynthesis in Silico. Understanding Complexity from Molecules to Ecosystems, Springer Science+Business Media B.V., 2009, 978-1-4020-9236-7.
[5] Govindjee, et al., *Photosystem II*, Encyclopedia of Life Sciences, John Wiley & Sons, 2010, pp. 1–15, https://doi.org/10.1002/9780470015902.a0000669.pub2.
[6] G.R. Fleming at al, Quantum effects in biology, Procedia Chem. 3 (2011) 38–57, https://doi.org/10.1016/j.proche.2011.08.011.
[7] H.M. Kalaji, et al., The use of chlorophyll fluorescence kinetics Analysis to Study the Performance of photosynthetic Machinery in plants, ch. 15, in: P. Ahmad (Ed.), Emerging Technologies and Management of Crop Stress Tolerance, vol. 2, Elsevier Inc., 2014, pp. 347–384, 10.1016.B978-0-12-800875-1.00015-6.
[8] I. Eisenberg, et al., Regulating the energy flow in a cyanobacterial light-harvesting antenna complex, J. Phys. Chem. B121 (2017) 1240–1247, https://doi.org/10.1021/acs.jpcb.6b10590.
[9] A. Stirbet, et al., Photosynthesis: basics, history and modeling, Ann. Bot. 126 (2020) 511–537, https://doi.org/10.1093/aob/mcz171.
[10] M.Y. Gorbunov, P.G. Falkowski, Using Chlorophyll fluorescence kinetics to determine photosynthesis in aquatic ecosystems, Limnol. Oceanogr. 9999 (2020) 1–13, https://doi.org/10.1002/lno.11581.
[11] H. Qiang, Y. Zarmi, A. Richmond, Combined effects of light intensity, light-path and culture density on output rate of *Spirulina platensis (Cyanobacteria)*, Eur. J. Phycol. 33 (1998) 165–171, https://doi.org/10.1080/09670269810001736663.
[12] H. Qiang, et al., Ultrahigh-cell-density culture of a marine green alga, Chlorococcum littorale in a flat-plate bioreactor, Appl. Microbiol. Biotechnol. 49 (1998) 655–662, https://doi.org/10.1007/s002530051228.
[13] A. Richmond, Z. Cheng-Wu, Y. Zarmi, Efficient use of strong light for high photosynthetic productivity: interrelationship between the optical path, the optimal population density and cell-growth inhibition, Biomol. Eng. 20 (2003) 229–236, https://doi.org/10.1016/S1389-0344(03)00060-1.
[14] M. Janssen, et al., Photosynthetic efficiency of *Dunaliella tertiolecta* under shirt light/dark cycles, Enzyme and Microb, Technol. 29 (2001) 298–305, https://doi.org/10.1016/S0141-0229(01)00387-8.
[15] C. Vejrazka, et al., Photosynthetic efficiency of chlamydomonas reinhardtii in flashing light, Biotechnol. Bioeng. 108 (2011) 2905–2913, https://doi.org/10.1002/bit.23270.
[16] S. Sforza, et al., Adjusted light and dark cycles can optimize photosynthetic efficiency in algae growing in photobioreactors, PLoS One 7 (2012) e38975, https://doi.org/10.1371/journal.pone.0038975.
[17] C. Vejrazka, et al., Photosynthetic efficiency of *Chlamydomonas reinhardtii* in attenuated, flashing light, Biotechnol. Bioeng. 109 (2012) 2567–2574, https://doi.org/10.1002/bit.24525.
[18] C. Vejrazka, et al., Photosynthetic efficiency and oxygen evolution of *Chlamydomonas reinhardtii* under continuous and flashing light, Appl. Microbiol. Biotechnol. 97 (2013) 1523–1532, https://doi.org/10.1007/s00253-012-4390-8.
[19] D. Simionato, et al., Optimization of light use efficiency for biofuel production in algae, Biophys. Chem. 182 (2013) 71–78, 10.106/j.bpc.2013.06.017.
[20] C. Vejrazka, et al., The role of an electron pool in algal photosynthesis during sub-second light-dark cycling, Algal Res. 12 (2015) 43–51, https://doi.org/10.1016/j.algal.2015.07.017.
[21] Y. Zarmi, et al., Enhanced algal photosynthetic photon efficiency by pulsed light, iScience 23 (2020) 101115, 10/106/j.isci.2020.101115.
[22] O. Habiby, et al., Exergy efficiency of light conversion into biomass in the macroalga Ulva sp. (Chlorophyta) cultivated under the pulsed light in a photobioreactor, Biotechnol. Eng. 115 (2018) 1694–1704, https://doi.org/10.1002/bit.26588.
[23] A. Richmond, H. Qiang, Handbook of Microalgal Culture: Applied Phycology and Biotechnology, 2n Edition, Wiley-Blackwell, 2013.
[24] A.M. Vera-Vibes, G. Perin, T. Morosinto, High-resolution photosynthesis -irradiance curves in microalgae, Bioenerg. Commun. 19 (2022) 1–8, https://doi.org/10.26124/bec:2022-0019, 2022.
[25] L.A. Franklin, M.R. Badger, A comparison of photosynthetic electron transport in macroalgae, measured by pulse amplitude modulated chlorophyll fluorometry and mass spectrometry, J. Phycol. 37 (2001) 756–767, https://doi.org/10.1045/j.1529-8817.2001.00156.x.
[26] J. Masojídek, et al., Photosystem II electron transport rates and oxygen production in natural waterblooms of freshwater cyanobacteria, J. Plankton Res. 23 (2001) 57–66, https://doi.org/10.1093/plankt/23.1.57.
[27] B.J. Longstaff, et al., An in situ study of photosynthetic oxygen exchange and electron transport rate in the marine macroalga Ulva lactuca (Chlorophyta), Photosynth. Res. 74 (2002) 281–293, https://doi.org/10.1023/A:1021279627409.
[28] F.L. Figueroa, R. Conede-Ávarez, I. Gómez, Relations between electron transport and rates determined by pulse amplitude modulated chlorophyll fluorescence and oxygen evolution in macroalgae under different light conditions, Photosynth. Res. 75 (2003) 259–275, https://doi.org/10.1023/A:1023936313544.

[29] P. Cardol, G. Forti, G. Finazzi, Regulation of electron transport in microalgae, Biochim. Biophys. Acta 1807 (2011) 912–918, https://doi.org/10.1016/j.bbabio.2010.12.004.
[30] Z.P. Ye, et al., A mechanistic model for the photosynthesis-light response based on the photosynthetic electron transport of Photosystem II, New Phytol. 199 (2013) 110–120, https://doi.org/10.1111/nph.12242.
[31] B. Diner, D. Mauzerall, The turnover of photosynthesis and Redox properties of the pool of electron carriers between the photosystems, Biochim. Biophys. Acta 305 (1973) 353–363, https://doi.org/10.1016/0005-2728(73)90181-3.
[32] E. Greenbaum, The turnover times and pool sizes of photosynthetic hydrogen production by green algae, Sol. Energy 23 (1979) 315–320, https://doi.org/10.1016/0038-092X(79)90125-7.
[33] S.W. McCauley, A. Melis, Quantitation of plastoquinone photoreduction in spinach chloroplasts, Photosynth. Res. 8 (1986) 3–16, https://doi.org/10.1007/BF00028472.
[34] J.E. Guenther, J.A. Nemson, A. Melis, Photosystem stoichiometry and chlorophyll antenna size in *Dunaliella salina* (green algae), Biochim. Biophys. Acta 934 (1988) 108–117, https://doi.org/10.1016/0005-2728(88)90125-9.
[35] O. Joliot, A. Joliot, Quantification of the electrochemical proton gradient and activation of ATP synthase in leaves, Biophys. Acta 1777 (2008) 676–683, https://doi.org/10.10126/j.bbabio.2008.04.010.
[36] R.E. Cleland, Voltammetric measurement of the plastoquinone redox state in isolated thylakoids, Photosynth. Res. 58 (1998) 183–192, https://doi.org/10.1023/A:1006165501184.
[37] D. Mauzerall, N.L. Greenbaum, The absolute size of a photosynthetic unit, Biochim. Biophys. Acta 974 (1989) 119–140, https://doi.org/10.1016/S0005-2728(89)80365-2.
[38] P.W. Hemelrijk, H.J. van Gorkom, Size-distributions of antenna and acceptor-pool of Photosystem II, Biochim. Biophys. Acta 1274 (1996) 31–38, https://doi.org/10.1016/0005-2728(96)00006-0.
[39] S.S. Hasan, W.A. Carmer, On rate limitations of electron transfer in the photosynthetic cytochrome b6f complex, Phys. Chem. Chem. (2012) 13853–13860, https://doi.org/10.1039/C2CP41386H.
[40] S. Malkin, et al., Photosystem II photosynthetic unit sizes from fluorescence induction in leaves, Plant Physiol. 67 (1981) 570–579, https://doi.org/10.1104/pp.67.3.570.
[41] A.C. Ley, Effective absorption cross-sections in *Porphyridium cruentum*, Plant Physiol. 74 (1984) 451–454, https://doi.org/10.1104/pp.74.2.451.
[42] N.L. Greenbaum, et al., Use of a light-induced respiratory transient to measure the optical cross-section of photosystem I in chlorella, Plant Physiol. 84 (1987) 879–882, https://doi.org/10.1104/pp.84.3.879.
[43] S. Falk, et al., Photosynthetic performance and fluorescence in relation to antenna size and absorption cross-sections in rye and barley grown under normal intermittent light conditions, Photosynth. Res. 42 (1994) 145–155, https://doi.org/10.1007/BF02187125.
[44] D.J. Sugget, et al., Evaluation of biophysical and optical determinations of light absorption by photosystem II in phytoplankton, Limnol Oceanogr. Methods 2 (2004) 316–332, https://doi.org/10.4319/lom.2004.2.316.
[45] T. de Marchin, et al., Analysis of PSII antenna size heterogeneity of *Chlamydomonas reinhardtii* during state transitions, Biochim. Biophys. Acta 1837 (2014) 121–130, https://doi.org/10.1016/j.bbabio.2013.07.009.
[46] C. Klughammer, U. Schreiber, Apparent PS II absorption cross-section and estimation of mean PAR in optically thin and dense suspensions of Chlorella, Photosynth. Res. 123 (2015) 77–92, https://doi.org/10.1007/s11120-014-0040-6.
[47] E. Kim, et al., Multimeric and monomeric photosystem II supercomplexes represent structural adaptations to low- and high-light conditions, J. Biol. Chem. 295 (2020) 14537–14545, https://doi.org/10.1074/jbc.RA120.014198.
[48] S. Tietz, et al., Functional implications of photosystem II crystal formation in photosynthetic membranes, J. Biol. Chem. 290 (2015) 14091–14106, https://doi.org/10.1074/jbc.M114.619841.
[49] J.W. Goodman, Statistical Optics, Wiley, New York, 2015, 978-1-119-00945-0.
[50] M. Fox, Quantum Optics: an Introduction (Oxford Master Series in Physics), Oxford University Press, New York, 2006, 10 0198566735.
[51] A. Mahulkar, et al., A simple model for algal photosynthesis for better light utilization with flashing light, BioEnergy Res 16 (2023) (2022) 1801–1815, https://doi.org/10.1007/s12155-022-10538-7.